Level-2P Derived products from SWIM instrument of CFOSAT

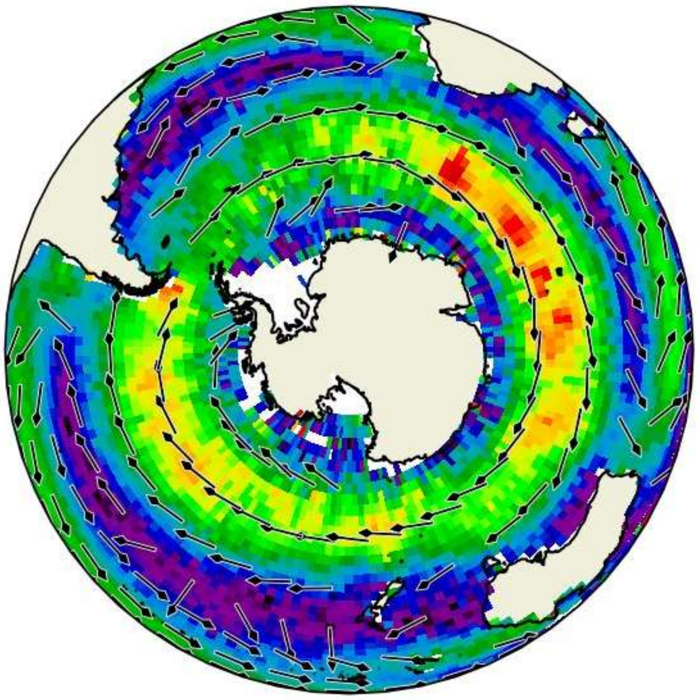

Nomenclature: SALP-MU-P-EA-23666-CLS

Issue:1.0

Date: September 2024

Chronology Issues:			
Issue:	Date:		Reason for change:
1.0	September 2024		Initial release - creation of the document

People involved in this issue:			
Written by:	Peureux Charles Averseng Matthias	CLS	Date : 2024/10/10
APPROVED BY:	Danièle Hauser	LATMOS	Date : 2024/10/10

List of Acronyms

Aviso+	Archiving, Validation and Interpretation of Satellite Oceanographic data
CLS	Collecte, Localisation, Satellites
CNES	Centre National d'Etudes Spatiales
SLA	Sea Level Anomaly
DAC	Dynamical atmospheric correction
L2	Level-2 product
L2P	Level-2+ product
L3	Level-3 product

Table of Contents

1. Introduction

This user manual describes the added value products estimated from CFOSAT SWIM instrument (L2PDER).

Dedicated to users unfamiliar with the mission, L2P products are added value products giving access to the largest community of users, including model assimilation actors.

In synergy with the needs of the WAVE-TAC (Thematic Assembly Centre), one of the eight TAC of the Copernicus Marine Environment Monitoring Service (CMEMS) project, SWIM L2P products intends to be an easy-to-ingest product, with comparable metrics.

The purpose of this document is to describe the specific Level-2P products derived (L2PDER) from SWIM instrument of CFOSAT. The instrument technology provides information from both Nadir and off-nadir.

The generation of those products is part of the FRench Oceanographic Ground Segment (FROGS) of the CFOSAT Mission. The dissemination of those products is part of the CNES Aviso+ web site.

After a description of the input data, a short overview of the processing steps is presented. Then complete information about user products is provided, giving nomenclature, format description, and software routines.

1.1 Data Policy and conditions of use

The product from CFOSAT L2PDER file is available free of charge for scientific studies and commercial activities.

2. Overview

1.2 SWIM directional spectra of ocean waves from off-nadir observations

SWIM (Surface Waves Investigation and Monitoring instrument) is one of CFOSAT's radar instruments. It is a wave scatterometer operated at near-nadir incidences: 0° (nadir), 2°, 4°, 6°, 8° and 10° (Figure 1). The three beams with the largest incidence angle (6°, 8° and 10°) provide the 2D surface ocean wave spectra.

Among these, the 10° incidence beam was shown to be the most reliable and has been selected for dissemination of off-nadir information at this stage of the project CalVal studies (see Hauser D. et al., 2021 and Peureux C., 2021).

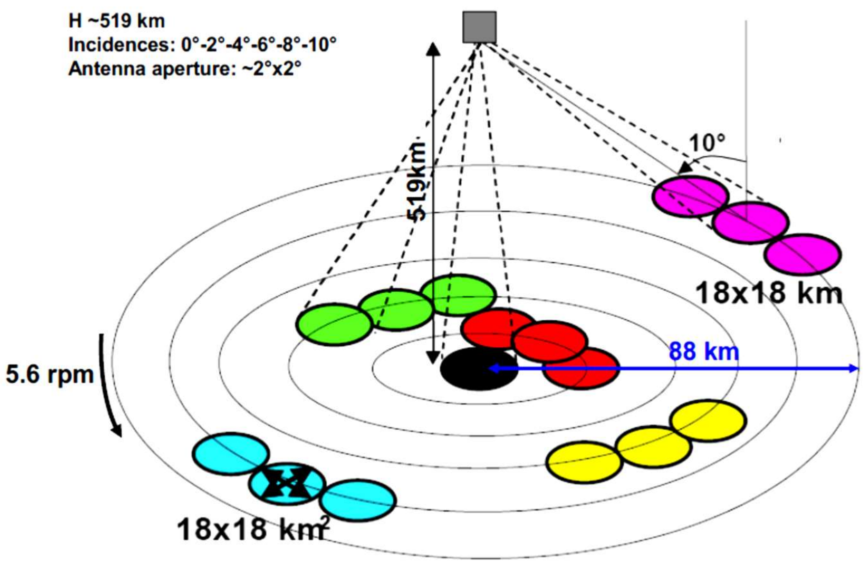

Figure 1. SWIM scatterometer

The principle of measurements is the following (see Hauser D. et al., 2017 for details). At the near-nadir incidence angles used by SWIM the transmitted signal is reflected by the sea surface towards the satellite thanks to a quasi-specular reflection generated by the presence of small facets (short waves). This quasi-specular backscattered signal is modulated within each footprint by the ocean waves (tilting effects by the presence of long waves). The maximum of modulation occurs for look angles close to the wave propagation direction. To the first order, these signal modulations are proportional to the slopes of the long waves. This allows estimations of the wave slope spectrum from the signal modulation spectrum (after correcting for speckle contamination) in each look direction. The wave spectrum is estimated from the modulation spectrum using a Modulation Transfer Function (MTF).

As the SWIM antenna continuously scans over 360°, the two-dimensional spectrum (in wave-number k and direction φ) can be derived by combining different look directions.

To build these directional wave spectra, off nadir boxes of about 90 x 70 km on each side of the satellite track (see Figure 2) are defined. The boxes include all azimuth in the range [0-180°] or [180°-360°]. The wave spectra are expressed as wave slope spectra in a $k-\varphi$ space with an ambiguity of ±180° in the propagation direction. Three main parameters are associated to these wave spectra: significant wave height, dominant wavelength, and dominant direction.

A 2D spectrum may contain information from multiple wave systems, for example, swell or wind sea. By defining different regions of the spectrum in the $k-\varphi$ space (i.e., partitions), one can extract the wave partitions and their properties (significant wave height, wavelength, direction).

For more details about how SWIM measures the 2D density spectrum of waves (see Hauser D. et al., 2017).

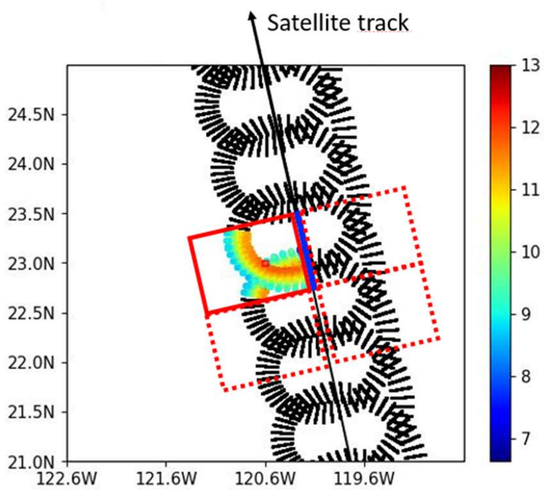

Figure 2. Example of a SWIM Off-nadir box (red solid box 90km wide/70km long) to the left of the satellite track, together with the associated nadir "box" (blue line along the track).

1.3 Orbits, Passes and Repeat cycle

'Orbit' is one revolution around the Earth by the satellite.

'Repeat Cycle' is the time period that elapses until the satellite flies over the same location again.

For CFOSAT:

- The orbit is sun-synchronous with an ascending pass at the equator around 7:00;
- The inclinaison is 97.465 deg;
- The passes are numbered from 1 to 394 representing a full 'repeat cycle' for the repetitive orbit;

- The repeat cycle is 13 days, meaning that the same path is covered (within ± 20 km) every 13 days.

The localisation of orbits (for realised and extrapolated cycles) can be found on the AVISO+ web site:

https://www.aviso.altimetry.fr/en/data/tools/pass-locator.html

2 Processing

2.1 Stokes drift for a generic wave spectrum

The Stokes drift is the lagrangian mean flow vector under the action of surface waves solely. It is mostly significant at the ocean surface, but can be significant down to a few tens of meters below the surface. Under the deep water approximation, it can be readily estimated at a depth z from the 2D spectrum of sea surface elevation $E(k,\varphi)$ (Kenyon, 1969):

$$\boldsymbol{U}_S(z) = 2\sqrt{g}\int_0^\infty k^{\frac{3}{2}}e^{2kz}\left[\int_0^{2\pi} E(k,\varphi)\boldsymbol{u}\, kd\varphi\right] dk \qquad (1),$$

where $\boldsymbol{u} = [\cos\varphi, \sin\varphi]^T$ is the unit vector in the direction of wave propagation, $E(k,\varphi)$ is defined such that the omni-directional wave height spectrum is

$$E(k) = \int_0^{2\pi} d\varphi\, k\, E(k,\varphi)$$

And the significant wave height H_S is :

$$H_S = 4\sqrt{\int_K E(k)dk} = 4\sqrt{\iint dk\, d\varphi k E(k,\varphi)} \qquad (2)$$

It also important to notice that:

- z is defined positive upwards, so that $z = 0\ m$ corresponds to the sea surface and $z = -15\ m$ corresponds to 15 meters below the surface
- $E(k,\varphi)$ is here expressed in the oceanographic convention, especially φ corresponds to the direction *towards* which waves or moving.
- g, the gravitational force, is approximated by $9.8\ m/s^2$.
- The deep water approximation restricts the application of this formula to water depths typically greater than half the dominant waves length, for which a shallow water correction should be applied.

2.2 Stokes drift for a parametric wind-sea spectrum

Wind-sea spectra have a regular shape as a function of a few sea-state parameters. One of them is provided by Pierson and Moskowitz (Pierson, 1964):

$$E(k) = \frac{\alpha_p}{2}k^{-3}\exp\left[-\frac{5}{4}\left(\frac{k_p}{k}\right)^2\right] \qquad (3)$$

α_p is the Phillips constant and k_p is the wind-sea peak wavenumber. According to a later reformulation by Elfouhaily et al. (Elfouhaily, 1997), for a wind-sea, the actual peak wave number differs from the theoretical peak wave-number $k_0 = g/U_{10}^2$ by the inverse wave age Ω:

$$k_p = k_0\Omega^2$$

The spectral shape **(3**) is represented on Figure 3. For Stokes drift computations especially, this spectral shape can be approximated by (Breivik O. J., 2014):

$$E(k) = \begin{cases} \frac{\alpha_p}{2}k^{-3}, k \geq k_p \\ 0, k < k_p \end{cases} \qquad (4)$$

Elfouhaily et al. mentioned a dependency of the Phillips constant α_p on wave age :

$$\alpha_p = 6 \times 10^{-3}\sqrt{\Omega} \qquad (5)$$

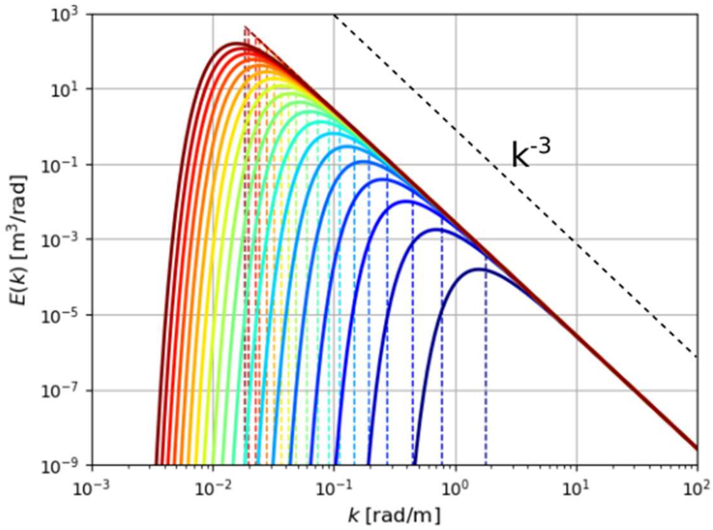

Figure 3: the Pierson-Moskowitz 1D wind-sea spectrum (solid, equation *(3)*) and its approximation (dashed, equation *(4)*) for fully developed seas ($\Omega = 0.84$) and wind speeds varying between 2 (blue),3,… and 20 m/s (red).

This spectral shape is interesting especially for the waves with wave number greater than a few times the peak wave number, because it accounts for the well-known observation that the wave number spectrum decreases as k^{-3} in this domain (Phillips, 1958).

To get the full 2D spectrum, the directional distribution of waves M is required:

$$\boldsymbol{E(k,\varphi)} = \frac{\boldsymbol{E(k)M(k,\varphi)}}{\boldsymbol{k}} \qquad (6)$$

$M(k,\varphi)$ is the directional spectrum such that

$$\int_0^{2\pi} d\varphi\, M(k,\varphi) = 1$$

Although Breivik et al. (Breivik O. J., 2014) used the same approximation as ours for the 1D spectrum, equation ***(4)***, they did not properly take directionality effects into account. Here, an Elfouhaily-like directional distribution (Elfouhaily, 1997) is assumed:

$$\boldsymbol{M(k,\varphi)} = \frac{\boldsymbol{1}}{\boldsymbol{\pi}}[\boldsymbol{1} + \boldsymbol{\Delta(k)}\cos \boldsymbol{2(\varphi - \varphi_w)}]\boldsymbol{H}[\cos(\boldsymbol{\varphi - \varphi_w})] \qquad (7)$$

where

$$H(x) = \begin{cases} 0 \; if \; x \leq 0 \\ 1 \; if \; x > 0 \end{cases}$$

and $\Delta(k)$ is a spreading function. Following Elfouhaily et al. again, this spreading function can be expressed as:

$$\Delta(k) = \tanh(a_0 + a_1 k^{-1.25}) \qquad (8)$$

Strictly speaking, this expression also differs from the one of Elfouhaily et al. as the ocean waves energy is assumed not to propagate against the wind. For convenience, it is possible to approximate *(7)* by:

$$\Delta(k) = \begin{cases} a_0 + a_1 k^{-1.25} \; if \; k \geq k_L \\ 1 \; if \; k < k_L \end{cases} \qquad (9)$$

where

$$a_0 = \frac{\ln 2}{4}$$

$$a_1 = a_p k_p^{1.25}$$

(10)

$$a_p = 4$$

and

$$k_L = \left(\frac{1 - a_0}{a_1}\right)^{-0.8} = \beta k_p$$

with

$$\beta = \left(\frac{1 - a_0}{a_p}\right)^{-0.8} = 3.53$$

(11)

This expression can be understood as the splitting of the waves directionality into two domains. The first domain between $k = k_p$ and $k = 3.53k_p$ is the one for which the waves are close to the dominant wavelength and almost unidirectional. The second for $k > 3.53k_p$is the one for which the wave field spreads out progressively, which is also observed in field measurements (Peureux, 2018).

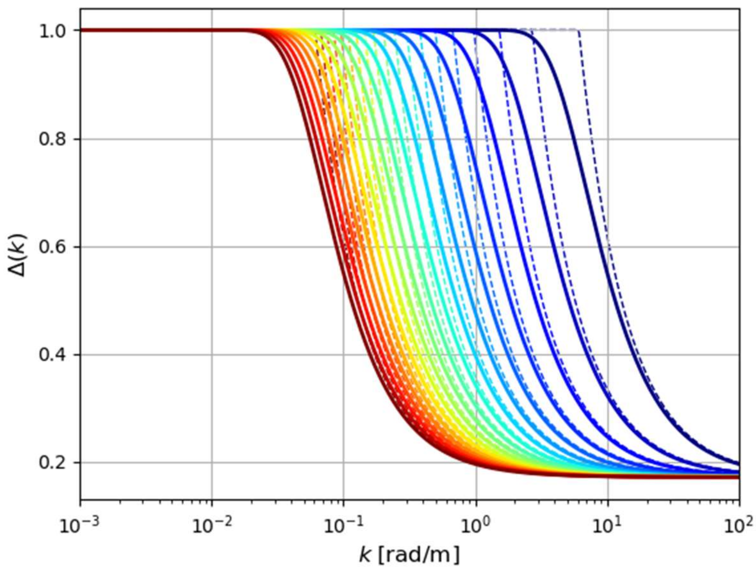

Figure 4 : Elfouhaily wind-sea spreading function (solid, equation *(8(3)*) and its approximation (dashed, equation *(9(4)*) for fully developed seas ($\Omega = 0.84$) and wind speeds varying between 2 (blue),3,… and 20 m/s (red).

It is then possible to compute the Stokes drift vector

$$\boldsymbol{U_s}(\mathrm{z}) = 2\sqrt{g}\int_0^\infty k^{\frac{3}{2}} e^{2kz}\left[\int_0^{2\pi} E(k,\varphi)\boldsymbol{u}\, kd\varphi\right] dk$$

associated with this parametric spectrum by combining ***(4)***, $\boldsymbol{E}(\boldsymbol{k})\boldsymbol{M}(\boldsymbol{k},\boldsymbol{\varphi})\boldsymbol{k}$ ***(***
6), ***(7)*** and ***(9)***. The algebra is lengthy, and only the main computation steps are detailed.

The Stokes drift can be written as an integral over wave numbers:

$$\boldsymbol{U_S}(z) = U_S(z)\boldsymbol{u}_w$$

where $\boldsymbol{u}_w$is the unit vector in the wind direction

$$U_S(z) = 2\sqrt{g}\int_0^\infty dk\, k^{\frac{3}{2}}E(k)m_1(k)e^{2k}$$

and

$$m_1(k) = \int_0^{2\pi} d\varphi \cos\varphi\, M(k,\varphi)$$

(12)

In Breivik et al. (Breivik O. J., 2014), an approximate profile was computed with the same assumptions as ours (called Phillips in their paper), except that it is assumed that $m_1(k) = 1$, i.e. that all waves travel in the same direction. Peureux et al. (Peureux, 2018) showed that directionality has a significant contribution to Stokes drift, thus in what follows, Breivik et al. computations are extended to the Elfouhaily-like directional spectrum *(7)*:

$$m_1(k) = \frac{2}{\pi}\left[1 + \frac{\Delta(\mathrm{k})}{3}\right]$$

(13)

Then, the Stokes drift using the approximation of $\Delta(k)$ ***(9)*** and the 1D spectrum ***(4)*** is

$$U_S(z) = \frac{2\alpha_p\sqrt{g}}{\pi}\int_{k_p}^\infty dk\, k^{-\frac{3}{2}}\left[1 + \frac{\Delta(\mathrm{k})}{3}\right]e^{2kz}$$

$$\boldsymbol{U_S(z)} = \boldsymbol{\frac{2\alpha_p\sqrt{g}}{\pi}\left[\int_{k_p}^\infty dk\, k^{-\frac{3}{2}}e^{2kz} + \frac{1}{3}\int_{k_p}^\infty dk\, k^{-\frac{3}{2}}\Delta(k)e^{2kz}\right]}$$

(14)

The following integrals will be useful:

$$I_1(k_a z) = \frac{\sqrt{k_a}}{2}\int_{k_a}^\infty dk\, k^{-\frac{3}{2}}e^{2kz} = e^{2k_a z} - \sqrt{-2\pi k_a z}\,\mathrm{erfc}\sqrt{-2k_a z}$$

(15)

$$I_2(k_a z) = \frac{7k_a^{7/4}}{4}\int_{k_a}^\infty dk\, k^{-\frac{11}{4}}e^{2kz} = e^{2k_a z}\left(1 + \frac{8}{3}k_a z\right) + \frac{4}{3}(-2k_a z)^{7/4}\Gamma\left(\frac{1}{4}, -2k_a z\right)$$

(16)

where erfc is the complementary error function $\operatorname{erfc} x = 1 - \operatorname{erf} x$ with

$$\operatorname{erf} x = \frac{2}{\sqrt{\pi}} \int_0^x e^{-t^2} dt$$

$\Gamma(s, x)$ is the upper incomplete gamma function

$$\Gamma(s, x) = \int_x^\infty dt\, e^{-t} t^{s-1}$$

Functions I_1 and I_2 are represented on Figure 5.

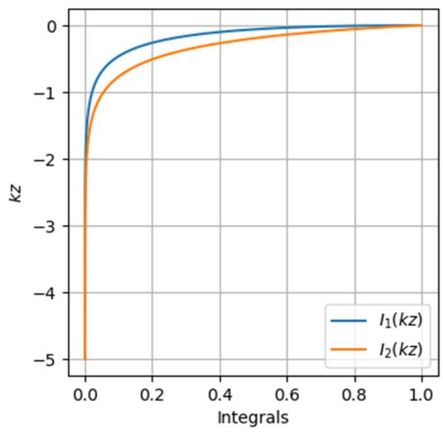

Figure 5: Integrals I_1 and I_2 from (15)**and** (16)

Then, the Stokes drift **(14)** can be expressed as a function of those two integrals **(15)** and **(16)**:

$$U_S(z) = \frac{4\alpha_p}{3\pi} c_p \left[4I_1(k_p z) + \sqrt{\frac{k_p}{k_L}} (a_0 - 1) I_1(k_L z) + \sqrt{\frac{k_p}{k_L}} \frac{2a_1}{7k_L^{5/4}} I_2(k_L z) \right]$$

(17)

where $c_p = \sqrt{g/k_p}$ is the dominant waves phase speed

If now the expressions for a_1, ***(10)*** and k_L, ***(11)***, are inserted into the Stokes drift expression (17), the Stokes drift is only a function of :

$$U_S(z) = \frac{16\alpha_p}{3\pi} c_p \left[I_1(k_p z) + \frac{a_0 - 1}{4\sqrt{\beta}} I_1(\beta k_p z) + \frac{a_p}{14} \beta^{-1/4} I_2(\beta k_p z) \right]$$

or

$$U_S(z) = 0.009 c_p [I_1(k_p z) - 0.11 I_1(3.53 k_p z) + 0.009 I_2(3.53 k_p z)]$$

(18)

for a fully developed sea ($\Omega = 0.84$).

In (18), the two first terms in the bracket are related to the omni-directional wave spectrum contribution whereas the last term (in I2) accounts for the contribution due to directionality.

This profile can be compared to the one proposed by Breivik et al. (Breivik O. J., 2014) which in the same wave age conditions writes:

$$U_S^P(z) = 2\alpha_p c_p I_1(k_p z)$$

Or, from ***(5)***:

$$U_S^P(z) = 0.011 c_p I_1(k_p z)$$

(19)

Both profiles are compared on Figure 6. They differ only slightly, remembering that the values here provided derive from theoretical values of a_0, a_p and β, provided in Elfouhaily et al. paper (Elfouhaily, 1997). In other words, more realistic values of those coefficients would lead to different vertical profiles, thus allowing for a wider diversity of behaviours.

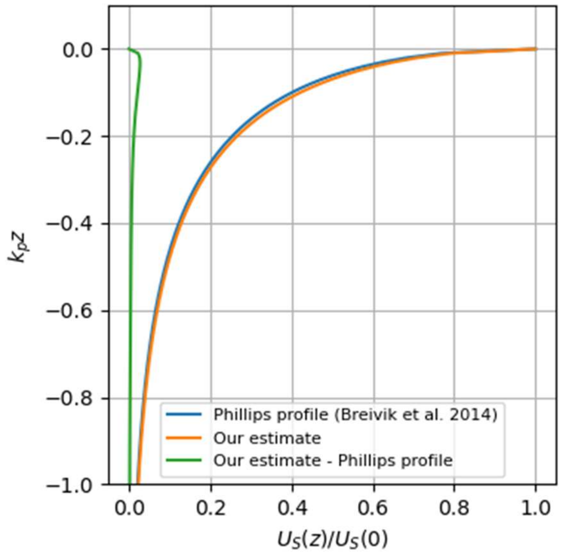

Figure 6 : Comparison of Stokes drift profiles from a Phillips spectrum (Breivik O. J., 2014), equation *(19)*-blue line, and our estimate, equation (18)-orange line. The green line is the difference between both.

2.3 Contribution of short waves to the Stokes drift from a parametric wind-sea spectrum

The previous derivation is useful to draw the ensemble picture of the Stokes drift profile under certain hypothesis. Now, for our purpose of applying it to operational use with SWIM, it is of interest to isolate the contribution of waves with wave numbers above a certain value k_{max} to the Stokes drift :

$$\boldsymbol{U}_S(z) = \boldsymbol{U}_S^L(z) + \boldsymbol{U}_S^S(z) \tag{20}$$

Where $U_S^L(z)$ is the contribution from waves longer than $\lambda_{max} = 2\pi/k_{max}$, and $U_S^S(z)$ of waves shorter. For SWIM, $U_S^L(z)$ can readily be estimated from SWIM spectra with $\lambda_{max} < 30\ m$ typically. It remains to estimate the shorter waves contribution based on the derivation of paragraph 'Stokes drift for a parametric wind-sea spectrum'. As it was the case in the previous paragraph, the short waves contribution is aligned with the wind:

$$\boldsymbol{U}_S^S(z) = U_S^S(z)\boldsymbol{u}_w$$

The short waves contribution to the Stokes drift writes:

$$U_S^S(z) = 2\sqrt{g}\int_{k_{max}}^{\infty} dk\, k^{\frac{3}{2}}E(k)m_1(k)e^{2kz} \tag{21}$$

The integration bounds will differ depending on the location of k_p and k_L relative to k_{max}. For this reason, let's define

$$k_0 = \max(k_{max}, k_p) \tag{22}$$

and

$$k_1 = \max(k_0, k_L) \tag{23}$$

The 3 possible cases are represented on Figure 7, and their corresponding sea-states on Figure 8.Three different cases are represented on Figure 7, that are distinguished by the position of the maximum wave number resolved by SWIM, kmax, with respect to the peak of the wind waves spectrum k_p and the transition wave number between long and short waves, $k_L = 3.53\ k_p$, defined in equation (11). In the case (a), neither the peak nor the transition of the wind-waves spectrum are resolved by SWIM. It corresponds typically, according to Figure 8, to young sea-states or to more mature sea-states for wind speeds below 5 m/s wind speed. The case (b) is intermediate while in the case (c), the whole wind-sea is resolved by SWIM.

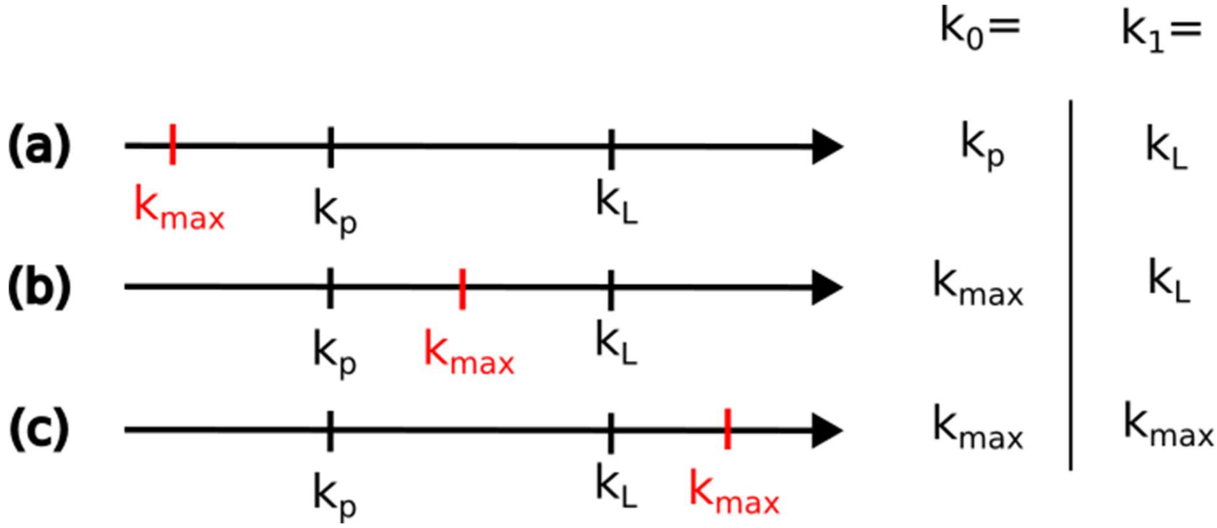

Figure 7 : 3 possible sea states for which the short waves contribution to Stokes drift differs qualitatively.

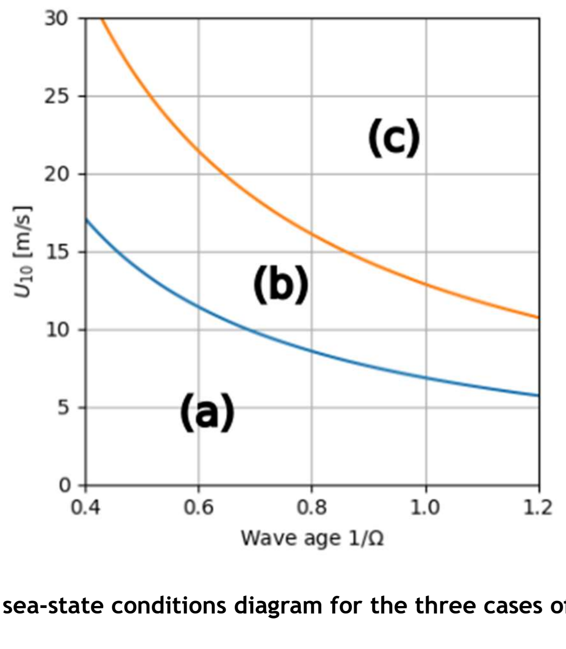

Figure 8 : sea-state conditions diagram for the three cases of Figure 7.

Then, **(21)** becomes

$$U_S^S(z) = 2\sqrt{g}\left[\int_{k_0}^{\infty} dk\, k^{-\frac{3}{2}} e^{2kz} + \frac{1}{3}\int_{k_0}^{k_1} dk\, k^{-\frac{3}{2}} e^{2kz} + \frac{1}{3}\int_{k_1}^{\infty} dk\, k^{-\frac{3}{2}} e^{2kz}\left(a_0 + a_1 k^{-5/4}\right)\right]$$

Including the expressions for I_1 and I_2, equations (**15**) and (**16**) leads to

$$\boxed{U_S^S(z) = \frac{16\alpha_p}{3\pi} c_0 \left\{ I_1(k_0 z) + \sqrt{\frac{k_0}{k_1}} \left[\frac{a_0 - 1}{4} I_1(k_1 z) + \frac{a_1}{14 k_1^{5/4}} I_2(k_1 z) \right] \right\}}$$

(24)

where

$$c_0 = \sqrt{\frac{g}{k_0}}$$

This expression can be further expressed as a function of sea-state (wave age and wind-speed) using the theoretical values of the coefficients a_0, a_1 and k_p from Elfouhaily et al.:

a) $k_{max} < k_p < k_L$:

$$U_S^S(z) = \frac{16\alpha_p}{3\pi} c_p \left\{ I_1(k_p z) + \beta^{-1/2} \left[\frac{a_0 - 1}{4} I_1(\beta k_p z) + \frac{a_p}{14\beta^{5/4}} I_2(\beta k_p z) \right] \right\}$$

b) $k_p < k_{max} < k_L$:

$$U_S^S(z) = \frac{16\alpha_p}{3\pi} c_{max} \left\{ I_1(k_{max} z) + \sqrt{\frac{k_{max}}{\beta k_p}} \left[\frac{a_0 - 1}{4} I_1(\beta k_p z) + \frac{a_p}{14\beta^{5/4}} I_2(\beta k_p z) \right] \right\}$$

c) $k_p < k_L < k_{max}$:

$$U_S^S(z) = \frac{16\alpha_p}{3\pi} c_{max} \left[\frac{a_0 + 3}{4} I_1(k_{max} z) + \frac{a_p}{14} \left(\frac{k_p}{\beta k_{max}} \right)^{5/4} I_2(k_{max} z) \right]$$

The correction **(24)** is plotted on Figure 9 and Figure 10.

At the surface (Fig.9), this correction can reach up to 9 cm/s in the young sea-state conditions at high wind conditions, i.e.it can contribute up to 40% to the total Stokes drift. However, it is less than 7 cm/s in mature and fully developed conditions. Note however that this correction is almost 0 already at $z = -3\ m$, (Fig 10).

Therefore, estimations of Stokes drift from SWIM data without corrections are representative of the value at some depth, whereas for estimation relative to the surface, corrections as described above and below must be applied. Using the method described below, we could estimate that the Stokes drift derived from SWIM without correction for the high frequency part is very well correlated to the Stokes drift given by the numerical wave model MFWAM at 15 m depth (see figures in Appendix in 8.2)

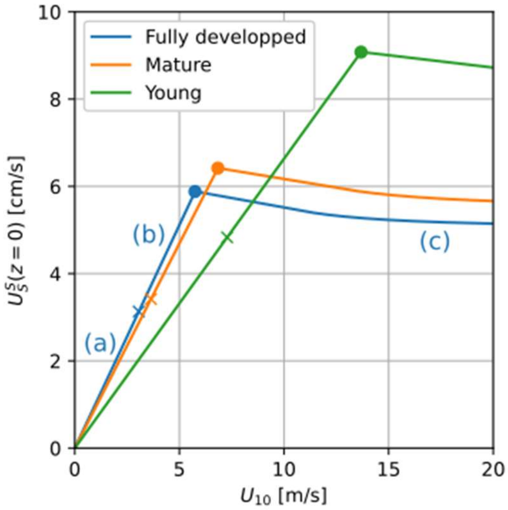

Figure 9: short waves contribution to the Stokes drift at the surface using theoretical values of a_0, a_p, k_p and α_p. The three cases of Figure 8 are delimited by a dot and a cross on each curve.

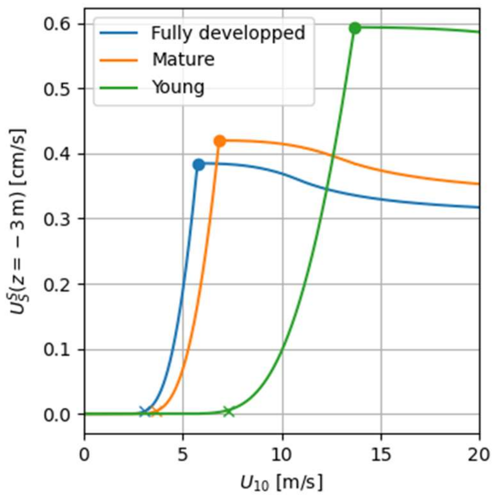

Figure 10 : short waves contribution to the Stokes drift at z=-3 m using theoretical values of a_0, a_p, k_p and α_p. The three cases of Figure 8 are delimited by a dot and a cross on each curve.

2.3.1 Practical estimation

In what follows, variables topped with a hat such as $\hat{x}$ denote their estimates, i.e. the estimate of x.

2.3.1.1 Disambiguation

First and foremost, the 180° ambiguity on SWIM spectra needs to be addressed. In fact, such symmetric spectra, input in a raw manner to Stokes drift formula such as $\boldsymbol{U}_S(z) = 2\sqrt{g}\int_0^{\infty} k^{\frac{3}{2}} e^{2kz}\left[\int_0^{2\pi} E(k,\varphi)\boldsymbol{u}\,kd\varphi\right] dk$ ***USz=*** $2\sqrt{g}\int_0^{\infty} k^{\frac{3}{2}} e^{2kz}\left[\int_0^{2\pi} E(k,\varphi)\boldsymbol{u}\,kd\varphi\right] dk$ *(1)*,

result in a null vector, as $m_1(k) = 0$. This is due to the fact that, for such spectra, the wave propagation direction has a 180° ambiguity. To solve this problem, an external wind vector is used (here from the colocated ECMWF model, present in the SWIM AWWAIS Level 2 products). An example of disambiguated spectrum is presented below on Figure 11.

In the L2PDER product, which is the subject of this note, it is applied directly on the 'pp_mean' variable relative to the beam 10°observations ° (the only ones kept in this product).

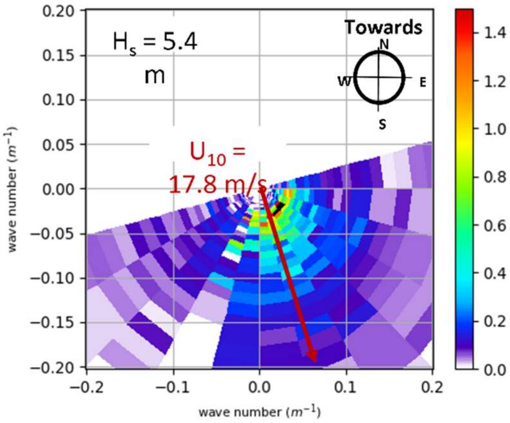

Figure 11 : example of disambiguated SWIM slopes spectrum using the external wind direction.

From now on, the disambiguated SWIM spectrum will be the reference spectrum for Stokes drift estimation. The resulting spectrum is normalized to check relationship ***(2)***. For example, in SWIM AWWAIS production up to number 6, this requires multiplying the spectrum resulting from disambiguation by 2.

2.3.1.2 Long waves contribution

According to the previous derivations, the Stokes drift is composed of a long waves and a short waves contribution, see equation (20). The long waves contribution can be readily estimated up to the limit of validity of SWIM spectra. In the present AWWAIS version, i.e. number 6, the SWIM wave vector extends to $k_{max} = 0.279\ rad/m$, corresponding to a wave length of 22.5 m.

First of all, the disambiguated SWIM slopes spectra, $S(k,\varphi)$ in m^2/rad, are converted to elevation spectra:

$$E(k,\varphi) = \frac{S(k,\varphi)}{k^2}$$

and input to equation $\boldsymbol{U_S}(z) = 2\sqrt{g}\int_0^{\infty} k^{\frac{3}{2}} e^{2kz}\left[\int_0^{2\pi} E(k,\varphi)\boldsymbol{u}\, kd\varphi\right] dk$ *(1)*, but restricted to the domain of definition of SWIM. The long waves contribution to the Stokes drift from SWIM spectra is:

$$\boldsymbol{U}_S^L(z) = \left\{2\sqrt{g}\sum_{i=1}^{N_k} k_i^{\frac{3}{2}} e^{2k_i z}\left[\sum_{j=1}^{N_\varphi} k_i \Delta\varphi_j \begin{vmatrix}\cos\varphi_j \\ \sin\varphi_j\end{vmatrix} E(k_i,\varphi_j)\right]\Delta k_i\right\}$$

2.3.1.3 Short waves contribution

The short waves contribution is as much as possible estimated from the existing data. A contribution of the type of equation **(24)** is chosen, which requires estimating the tail level, i.e. the Phillips constant α_p, and the directional coefficients a_0 and a_1 from the behavior of $m_1(k)$.

2.3.1.3.1 Tail level estimate

Following the model for the Phillips spectrum ***(4)***, the omni-directional elevation spectrum should follow a k^{-3} law:

$$E(k) = \frac{\alpha_p}{2} k^{-3}$$

where α_p enters the expression for the Stokes drift from short waves. α_p is estimated using the 5 last points of the tail:

$$\hat{\alpha}_p = 2\exp\left\{\frac{1}{5}\sum_{i=N_k-4}^{N_k} \ln\left[E(k_i)k_i^{-3}\right]\right\} \quad (25)$$

An example is shown on Figure 12 of such prolongation based on this α_p estimate.

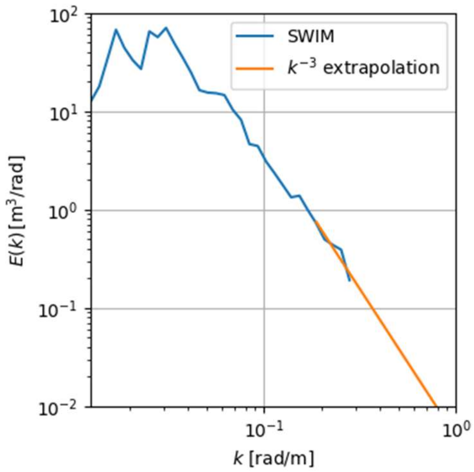

Figure 12: elevation spectrum prolongation example from SWIM using a Phillips constant estimate.

Several limitations of this algorithm can already be discussed:

- This prolongation is only valid above $k = k_p$, in other words if the spectral peak is resolved. This would, according to the growth laws taken from Elfouhaily et al. (Elfouhaily, 1997) correspond to the case (b) and (c) of Figure 8. This would not be the case for very young waves or for wind speeds below typically 5 m/s. In that case, this algorithm would either prolongate the tail based on noise and/or possibly present swells. Quantifying this error is hard but it is believed that this prolongation would not lead to a Stokes drift overestimation.
- More generally, the exponent -3 for the prolungation can be discussed. For example, Lenain and Pizzo (Lenain, 2020) argue that the k^{-3} part of the spectrum would be preceded by a $k^{-2.5}$ part. Such spectra would increase the Stokes drift by an amount that they quantified. The application of such procedure is thus judged too hard in the absence of a better resolution capability of the wind-sea by SWIM, with enough accuracy. Thus, it is chosen here to keep the fit with a k^{-3} law.

2.3.1.3.2 Directional estimate

This estimate is based on the fact that, from Elfouhaily spectrum, combining equations *(**9**)* and **(13)** :

$$m_1(k) \approx \gamma + \delta k^{-\frac{5}{4}} \tag{26}$$

at high enough wave numbers, where

$$\gamma = \frac{2}{\pi}\left(1 + \frac{a_0}{3}\right) \tag{27}$$

and

$$\delta = \frac{2a_1}{3\pi} \tag{28}$$

From which a_0 and a_1 can be deduced and used for Stokes drift estimate. In practice, these two parameters are estimated from a local linear fit of the directional integral $m_1(k)$ over the 5 last points resolved by SWIM, estimated from SWIM spectrum after disambiguation. First, the linear fitting parameters are determined such that

$$m_1(k) = \gamma_l + \epsilon_l k$$

Then, from a Taylor expansion of *(**5**)* around $\bar{k} = (1/5)\sum_{i=N_k-4}^{N_k} k_i$:

$$\hat{\delta} = -\frac{4\epsilon_l}{5}\bar{k}^{9/4}$$

$$\hat{\gamma} = \gamma_l + \frac{9\epsilon_l}{5}\bar{k}$$

and $\hat{a}_0$ and $\hat{a}_1$ are deduced from (27) and (28):

$$\hat{a}_0 = 3\left(\frac{\pi\hat{\gamma}}{2} - 1\right) \tag{29}$$

$$\hat{a}_1 = \frac{3\pi\hat{\delta}}{2} \tag{30}$$

An example of such estimate is provided on Figure 13.

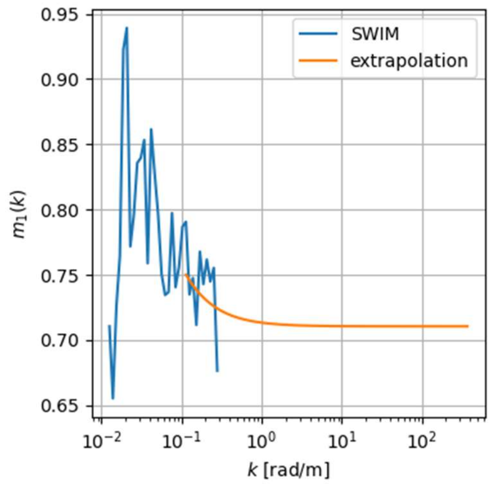

Figure 13 : example of directionality estimates and extrapolation from SWIM spectrum.

Several limitations of this algorithm can already be discussed:

- To keep $\Delta(k)$ positive for all values of k, the estimate of a_1 is clipped to
$$\hat{a}_1 = \begin{cases} \hat{a}_1 \; if \; \hat{a}_1 > -(\hat{a}_0 + 3)k_{max}^{-5/4} \\ -(\hat{a}_0 + 3)k_{max}^{-\frac{5}{4}} \; else \end{cases}$$
- Our tests based on SWIM spectra have shown that negative values of a1 are often found with this scheme. This is not geophysically consistent because from our knowledge of wave spectra, it is expected to be always positive, This is unlikely to be caused by real oceanographic signal, and consequently rather by noise. It might be a consequence of the increased speckle noise along SWIM track direction. a_1 estimates might then improve with SWIM products processing improvements.
- Assuming such a shape for m_1 (from equation (26))supposes that the wave number domain where the estimates are performed is above $\sim 3.53k_p$ (see case c in Figure 7 and Figure 8). This might lead to a slight error on the Stokes drift, either because the wind-sea peak is resolved but not caught by SWIM or because the directionality around the peak is underestimated. These errors are negligible as the weight of the directional terms in (**18**) is small compared to the first omnidirectional term.

2.3.1.3.3 Final estimate

Once the Phillips constant is estimated from (**25**) and the directional coefficients from (29) and (30), there still lacks a step to get the short wave contribution to the Stokes drift from (**24**). The first ingredient missing is to assume that

$$k_0 = k_1 = k_{max}$$

This corresponds to the case c of Figure 77 and 8, to be consistent with the assumptions made while performing the directionality estimate.

To summarize, the Stokes drift vector at a depth z is obtained:

1. By estimating the Phillips constant from SWIM omni-directional spectrum
2. By estimating directional coefficients from SWIM m1

3. By substituting the previous estimates in formula and assuming

$$k_0 = k_1 = k_{max}$$

3 SWIM Stokes drift products

3.1 Temporal availability

CFOSAT L2PDER files including SWIM Stokes drift products are available from the 25th of April 2019, corresponding to the upgrade of the CWWIC chain that corrected an error in the onboard processing of the spectral beams data, to 10th of January 2025. Prior and beyond that date, no reliable information is available.

3.2 Nomenclature

CFOSAT L2PDER filenames are named under CFOSAT L2 model:

CFO_OPXX_SWI_L2PDER_F_<begin_date>T<begin_hour>_<end_date>T<end_hour>.nc

Where the name components are:

- OPXX: where XX corresponds to the current version of the L2 products;
- <begin_date> under Year-Month-Day format: YYYYMMDD;
- <end_date> under Year-Month-Day format: YYYYMMDD;
- <begin_hour> under Hour-Minute-Second format: HHmmss;
- <end_hour> under Hour-Minute-Second format: HHmmss.

This is a filename example corresponding to the current OP06 L2 products:

CFO_OP06_SWI_L2PDER_F_20200101T021428_20200101T034845**.nc**

4 Data Format

This chapter presents the data storage format and convention used for Stokes drift products. All products are distributed in NetCDF-4 with norm CF. NetCDF (Network Common Data Form) is an open source, generic and multi-platform format developed by Unidata. An exhaustive presentation of NetCDF and additional conventions is available on the following web site:

https://www.unidata.ucar.edu/software/netcdf/

All basic NetCDF conventions are applied to files. Additionally, the files are based on the attribute data tags defined by the Cooperative Ocean/Atmosphere Reasearch Data Service (COARDS) and Climate Forecast (CF) metadata conventions. The CF convention generalises and extends the COARDS convention but relaxes the COARDS constraints on dimension and order and specifies methods for reducing the size of datasets. A wide range of software is available to write or read NetCDF/CF files. API made available by UNIDATA:

- C/C++/Fortran;
- Java;
- MATLAB, Objective-C, Perl, Python, R, Ruby, Tcl/Tk.

4.1 Dimensions

Several dimensions are defined in the L2PDER products:

- n_phi: number of azimuthal bins;
- n_box: number of boxes in the current file;
- n_posneg: refers to the left/right side of the track (n_posneg=2);
- nk: number of wavenumber bins;

4.2 Data Handling Variables

The variables defined in the product are listed and described in Table 1 for the nadir box related variables and Table 2 for the off-nadir variables. The corresponding L2 variable name is also provided for each L2PDER variable, as well as modifications from the original values in the L2 products, if any.

Name of variable	Type	Content	Unit	Dimensions	Name of equivalent L2 variable
time_nadir_l2	double	Time at the center of the nadir box with reference changed from 2009/01/01 to 2000/01/01	seconds since 2000-01-01 00:00:00 UTC	n_box	time_nadir_l2
lat_nadir_l2	int	Latitude of the center of the nadir box	degrees_north	n_box	lat_nadir_l2
lon_nadir_l2	int	Longitude of the center of the nadir box	degrees_east	n_box	lon_nadir_l2
nadir_swh_box	short	Nadir SWH compressed by nadir box	meters	n_box	nadir_swh_box
flag_valid_swh_box	byte	Quality flag for nadir_swh_box: 0: valid 1: invalid	none	n_box	flag_valid_swh_box
nadir_wind_box	short	Nadir wind speed value compressed by nadir box	meters / s	n_box	nadir_wind_box
flag_valid_wind_box	byte	Quality flag for nadir_wind_box: 0: valid 1: invalid	none	n_box	flag_valid_wind_box
phi_orbit_box	short	Angle between the orbit plane (i.e., track) and the geographical north	none	n_box	phi_orbit_box

Table 1 : Nadir box related variables

Name of variable	Type	Content	Unit	Dimensions	Name of equivalent L2 variable
time_spec_l2	double	Time at the center of the off-nadir box with reference changed from 2009/01/01 to 2000/01/01	seconds since 2000-01-01 00:00:00 UTC	n_posneg, n_box	time_spec_l2
lat_spec_l2	int	Latitude of the center of the off-nadir box	degrees_north	n_posneg, n_box	lat_spec_l2
lon_spec_l2	int	Longitude of the center of the off-nadir box	degrees_east	n_posneg, n_box	lon_spec_l2
k_spectra	short	Wave number vector (values at the center	1/meters	nk	k_spectra

		of the wave number bins) redefined for the 20-500 m wavelength range.			
phi_vector	short	Azimuth angle vector (values at the center of the azimuth angle bins), extended from [0°,180°] to [0°, 360°].	degrees	n_phi	phi_vector
swh_ecmwf	short	SWH from the ECMWF model data	meters	n_posneg, n_box	swh_ecmwf
u10_ecmwf	short	U wind speed from the ECMWF model data	meters/s	n_posneg, n_box	u10_ecmwf
v10_ecmwf	short	V wind speed from the ECMWF model data	meters/s	n_posneg, n_box	v10_ecmwf
pp_mean	Short	2D mean slope spectrum of the 10° incidence beam only and filtered of parasitic peaks.	meters^2 / radians	nk, n_phi, n_posneg, n_box	**pp_mean**
flag_valid_pp_mean	Byte	Quality flag on the 2D mean slope spectrum of the 10° incidence beam only.	none	nk, n_phi, n_posneg, n_box	none
eastward_stokes_drift_raw_0m	double	Eastward Stokes drift estimated at 0m depth from SWIM spectrum ([22.5-500] wavelength range).	Centimeters per second	n_posneg, n_box	none
northward_stokes_drift_raw_0m	Double	Northward Stokes drift estimated at 0m depth from SWIM spectrum ([22.5-500] wavelength range).	Centimeters per second	n_posneg, n_box	none
eastward_stokes_drift_raw_15m	Double	Eastward Stokes drift estimated at 15m depth from SWIM spectrum ([22.5-500] wavelength range).	Centimeters per second	n_posneg, n_box	none
northward_stokes_drift_raw_15m	Double	Northward Stokes drift estimated at 15m depth from SWIM spectrum ([22.5-500] wavelength range).	Centimeters per second	n_posneg, n_box	None
eastward_stokes_drift_full_0m	Double	Eastward Stokes drift estimated at 0m depth from the extended spectrum: SWIM spectrum ([22.5- 500] wavelength range) completed by an Elfouhaily modelling for largest wave numbers.	Centimeters per second	n_posneg, n_box	none
northward_stokes_drift_full_0m	Double	Northward Stokes drift estimated at 0m depth	Centimeters per second	n_posneg,	none

		from the extended spectrum: SWIM spectrum ([22.5- 500] wavelength range) completed by an Elfouhaily modelling for largest wave numbers.		n_box	
eastward_stokes_drift_full_15m	Double	Eastward Stokes drift estimated at 15m depth from the extended spectrum: SWIM spectrum ([22.5- 500] wavelength range) completed by an Elfouhaily modelling for largest wave numbers.	Centimeters per second	n_posneg, n_box	none
northward_stokes_drift_ full_15m	Double	Northward Stokes drift estimated at 15m depth from the extended spectrum: SWIM spectrum ([22.5- 500] wavelength range) completed by an Elfouhaily modelling for largest wave numbers.	Centimeters per second	n_posneg, n_box	none

Table 2 : Off-nadir variables

5 News, updates and reprocessing

5.1 Operational news

To be kept informed about events occurring on the satellites and on the potential services interruption, see the operational news on the Aviso+ website:

https://www.aviso.altimetry.fr/en/news/operational-news-and-status.html

5.2 Updates and reprocessing

5.2.1 SWIM L2PDER product version

The evolutions hereafter are listed hereafter :

Version	Delivery date	Period	FA	Evolution with respect to previous version
v1.0	2024-11-01	2019/04/25 - 2025/01/10		• Dataset creation including Stokes drift processing

5.3 Additional Data and Citation

Information about the starting dates of each cycle can be found at the following webpage under Localisation of Measurements:

https://www.aviso.altimetry.fr/en/missions/current-missions/cfosat.html

Any use of this dataset must cite its DOI 10.24400/527896/a01-2024.005 as well as the following sentence: "This Level-2P Derived product was produced by CLS in the frame of the FRench Oceanographic Ground Segment (FROGS) of the CFOSAT Mission and distributed by AVISO+ with the support of CNES."

6 Products policy and accessibility

The use of the CFOSAT L2PDER products is described in the AVISO+ License Agreement.

CFOSAT L2PDER products are available via authenticated servers:

- CNES AVISO FTP/SFTP access (with AVISO+ credentials):
  - ftp://ftp-access.aviso.altimetry.fr:21
  - ftp://ftp-access.aviso.altimetry.fr:2122
    - /cfosat_products/swim_l2p_stokes
- CNES AVISO THREDDS Data Server access (with AVISO+ credentials): https://tds-odatis.aviso.altimetry.fr/thredds/catalog/L2P/dataset-l2p-cfosat-swim-derived-products-stokes.html
- On the authenticated AVISO+ CNES Data Center (archived products): https://aviso-data-center.cnes.fr/

7 Contact

For more information, please contact:

Aviso+ User Services
E-mail: aviso@altimetry.fr
On Internet: https://www.aviso.altimetry.fr/

The user service is also interested in user feedbacks; questions, comments, proposals, requests are much welcome.

8 Appendix

8.1 Example of L2PDER product file

```
netcdf CFO_OP06_SWI_L2PDER_F_20200101T021428_20200101T034845 {
dimensions:
	n_phi = 24 ;
	n_box = 529 ;
	n_posneg = 2 ;
	nk = 32 ;
variables:
	double time_nadir_l2(n_box) ;
		time_nadir_l2:units = "seconds since 2000-01-01 00:00:00.0" ;
		time_nadir_l2:axis = "T" ;
		time_nadir_l2:standard_name = "time" ;
		time_nadir_l2:calendar = "gregorian" ;
		time_nadir_l2:long_name = "Mean time of box area (sec. since 2000-01-01)" ;
	double time_spec_l2(n_posneg, n_box) ;
		time_spec_l2:units = "seconds since 2000-01-01 00:00:00.0" ;
		time_spec_l2:axis = "T" ;
		time_spec_l2:standard_name = "time" ;
		time_spec_l2:calendar = "gregorian" ;
		time_spec_l2:long_name = "Mean time of 2D spectrum coverage area (sec. since 2000-01-01)"
;
	float lat_nadir_l2(n_box) ;
		lat_nadir_l2:_FillValue = 9.96921e+36f ;
		lat_nadir_l2:long_name = "Mean latitude of nadir beam in each box" ;
		lat_nadir_l2:references = "CF-GSFR-SP-807-CNES" ;
		lat_nadir_l2:source = "" ;
		lat_nadir_l2:units = "degrees_north" ;
		lat_nadir_l2:valid_min = -90.f ;
		lat_nadir_l2:valid_max = 90.f ;
		lat_nadir_l2:least_significant_digit = 3 ;
	float lon_nadir_l2(n_box) ;
		lon_nadir_l2:_FillValue = 9.96921e+36f ;
		lon_nadir_l2:long_name = "Mean longitude of nadir beam in each box" ;
		lon_nadir_l2:references = "CF-GSFR-SP-807-CNES" ;
		lon_nadir_l2:source = "" ;
		lon_nadir_l2:units = "degrees_east" ;
		lon_nadir_l2:valid_min = -180.f ;
		lon_nadir_l2:valid_max = 180.f ;
		lon_nadir_l2:least_significant_digit = 3 ;
	float lat_spec_l2(n_posneg, n_box) ;
		lat_spec_l2:_FillValue = 9.96921e+36f ;
		lat_spec_l2:long_name = "Mean latitude of 2D spectrum coverage area, in middle of the box" ;
		lat_spec_l2:references = "CF-GSFR-SP-804-CNES" ;
		lat_spec_l2:source = "" ;
		lat_spec_l2:units = "degrees_north" ;
		lat_spec_l2:valid_min = -90.f ;
		lat_spec_l2:valid_max = 90.f ;
		lat_spec_l2:least_significant_digit = 3 ;
	float lon_spec_l2(n_posneg, n_box) ;
		lon_spec_l2:_FillValue = 9.96921e+36f ;
		lon_spec_l2:long_name = "Mean longitude of 2D spectrum coverage area, in middle of the
box" ;
		lon_spec_l2:references = "CF-GSFR-SP-804-CNES" ;
		lon_spec_l2:source = "" ;
		lon_spec_l2:units = "degrees_east" ;
		lon_spec_l2:valid_min = -180.f ;
```

```
		lon_spec_l2:valid_max = 180.f ;
		lon_spec_l2:least_significant_digit = 3 ;
	float k_spectra(nk) ;
		k_spectra:_FillValue = 9.96921e+36f ;
		k_spectra:long_name = "Wave number vector" ;
		k_spectra:references = "CF-GSFR-SP-804-CNES" ;
		k_spectra:source = "" ;
		k_spectra:units = "m-1" ;
		k_spectra:valid_min = 0.f ;
		k_spectra:valid_max = 1.f ;
		k_spectra:least_significant_digit = 6 ;
	float phi_orbit_box(n_box) ;
		phi_orbit_box:_FillValue = 9.96921e+36f ;
		phi_orbit_box:long_name = "Angles between orbit plane and geographical North" ;
		phi_orbit_box:references = "CF-GSFR-SP-804-CNES" ;
		phi_orbit_box:source = "" ;
		phi_orbit_box:units = "radians" ;
		phi_orbit_box:valid_min = 0.f ;
		phi_orbit_box:valid_max = 7.f ;
		phi_orbit_box:least_significant_digit = 2 ;
	float nadir_swh_box(n_box) ;
		nadir_swh_box:_FillValue = 9.96921e+36f ;
		nadir_swh_box:long_name = "Swh value from nadir processing compressed by box" ;
		nadir_swh_box:references = "CF-GSFR-SP-807-CNES" ;
		nadir_swh_box:source = "" ;
		nadir_swh_box:units = "m" ;
		nadir_swh_box:valid_min = 0.f ;
		nadir_swh_box:valid_max = 100.f ;
		nadir_swh_box:least_significant_digit = 3 ;
	byte flag_valid_swh_box(n_box) ;
		flag_valid_swh_box:_FillValue = -127b ;
		flag_valid_swh_box:flag_meanings = "valid invalid" ;
		flag_valid_swh_box:flag_values = 0b, 1b ;
		flag_valid_swh_box:long_name = "Quality flag on swh value" ;
		flag_valid_swh_box:references = "CF-GSFR-SP-807-CNES" ;
		flag_valid_swh_box:source = "" ;
		flag_valid_swh_box:least_significant_digit = 0 ;
	float nadir_wind_box(n_box) ;
		nadir_wind_box:_FillValue = 9.96921e+36f ;
		nadir_wind_box:long_name = "Wind speed value from nadir processing compressed by box" ;
		nadir_wind_box:references = "CF-GSFR-SP-807-CNES" ;
		nadir_wind_box:source = "" ;
		nadir_wind_box:units = "m.s-1" ;
		nadir_wind_box:valid_min = 0.f ;
		nadir_wind_box:valid_max = 100.f ;
		nadir_wind_box:least_significant_digit = 3 ;
	byte flag_valid_wind_box(n_box) ;
		flag_valid_wind_box:_FillValue = -127b ;
		flag_valid_wind_box:flag_meanings = "valid invalid" ;
		flag_valid_wind_box:flag_values = 0b, 1b ;
		flag_valid_wind_box:long_name = "Quality flag on wind value" ;
		flag_valid_wind_box:references = "CF-GSFR-SP-807-CNES" ;
		flag_valid_wind_box:source = "" ;
		flag_valid_wind_box:least_significant_digit = 0 ;
	float swh_ecmwf(n_posneg, n_box) ;
		swh_ecmwf:_FillValue = 9.96921e+36f ;
		swh_ecmwf:long_name = "Significant wave height from ECMWF data" ;
		swh_ecmwf:references = "CF-GSFR-SP-804-CNES" ;
		swh_ecmwf:source = "" ;
		swh_ecmwf:units = "m" ;
		swh_ecmwf:valid_min = 0.f ;
		swh_ecmwf:valid_max = 50.f ;
		swh_ecmwf:least_significant_digit = 2 ;
	float u10_ecmwf(n_posneg, n_box) ;
		u10_ecmwf:_FillValue = 9.96921e+36f ;
		u10_ecmwf:long_name = "10 metres u wind speed from ECMWF data" ;
		u10_ecmwf:references = "CF-GSFR-SP-804-CNES" ;
```

```
		u10_ecmwf:source = "" ;
		u10_ecmwf:units = "m/s" ;
		u10_ecmwf:valid_min = -100.f ;
		u10_ecmwf:valid_max = 100.f ;
		u10_ecmwf:least_significant_digit = 2 ;
	float v10_ecmwf(n_posneg, n_box) ;
		v10_ecmwf:_FillValue = 9.96921e+36f ;
		v10_ecmwf:long_name = "10 metres v wind speed from ECMWF data" ;
		v10_ecmwf:references = "CF-GSFR-SP-804-CNES" ;
		v10_ecmwf:source = "" ;
		v10_ecmwf:units = "m/s" ;
		v10_ecmwf:valid_min = -100.f ;
		v10_ecmwf:valid_max = 100.f ;
		v10_ecmwf:least_significant_digit = 2 ;
	float phi_vector(n_phi) ;
		phi_vector:_FillValue = 9.96921e+36f ;
		phi_vector:valid_min = 0.f ;
		phi_vector:long_name = "Phi vector (center of bin)" ;
		phi_vector:least_significant_digit = 1LL ;
		phi_vector:units = "degree" ;
		phi_vector:valid_max = 360.f ;
		phi_vector:references = "CF-GSFR-SP-804-CNES" ;
		phi_vector:comment = "optionnelle" ;
		phi_vector:source = "" ;
	float pp_mean(nk, n_phi, n_posneg, n_box) ;
		pp_mean:_FillValue = 9.96921e+36f ;
		pp_mean:long_name = "Best 2D mean slope spectrum for spectral beam 10 degrees" ;
		pp_mean:least_significant_digit = 3LL ;
		pp_mean:valid_max = 100.f ;
		pp_mean:units = "m^2 / radians" ;
		pp_mean:references = "CF-GSFR-SP-804-CNES" ;
		pp_mean:comment = "optionnelle" ;
	byte flag_valid_pp_mean(nk, n_phi, n_posneg, n_box) ;
		flag_valid_pp_mean:_FillValue = -127b ;
		flag_valid_pp_mean:long_name = "validation flag for the 2D mean slope spectrum for spectral
beam 10 degrees (all criteria)" ;
		flag_valid_pp_mean:flag_values = 0b, 1b ;
		flag_valid_pp_mean:flag_meanings = "valid invalid" ;
	float northward _stokes_drift_raw_0m (n_posneg, n_box) ;
		northward _stokes_drift_raw_0m:_FillValue = 9.96921e+36f ;
		northward _stokes_drift_raw_0m:long_name = "Northward Stokes drift estimated at 0m depth
from SWIM spectrum ([22.5-500] wavelength range)." ;
		northward _stokes_drift_raw_0m:least_significant_digit = 3LL ;
		northward _stokes_drift_raw_0m:units = "cm/s" ;
		northward _stokes_drift_raw_0m:comment = "optionnelle" ;
	float eastward_stokes_drift_raw_0m (n_posneg, n_box) ;
		eastward_stokes_drift_raw_0m:_FillValue = 9.96921e+36f ;
		eastward_stokes_drift_raw_0m:long_name = " Eastward Stokes drift estimated at 0m depth
from SWIM spectrum ([22.5-500] wavelength range)." ;
		eastward_stokes_drift_raw_0m:least_significant_digit = 3LL ;
		eastward_stokes_drift_raw_0m:units = "cm/s" ;
		eastward_stokes_drift_raw_0m:comment = "optionnelle" ;
	float northward _stokes_drift_raw_15m (n_posneg, n_box) ;
		northward _stokes_drift_raw_15m:_FillValue = 9.96921e+36f ;
		northward _stokes_drift_raw_15m:long_name = "Northward Stokes drift estimated at 15m
depth from SWIM spectrum ([22.5-500] wavelength range)." ;
		northward _stokes_drift_raw_15m:least_significant_digit = 3LL ;
		northward _stokes_drift_raw_15m:units = "cm/s" ;
		northward _stokes_drift_raw_15m:comment = "optionnelle" ;
	float eastward _stokes_drift_raw_15m (n_posneg, n_box) ;
		eastward _stokes_drift_raw_15m:_FillValue = 9.96921e+36f ;
		eastward _stokes_drift_raw_15m:long_name = "Eastward Stokes drift estimated at 15m depth
from SWIM spectrum ([22.5-500] wavelength range)." ;
		eastward _stokes_drift_raw_15m:least_significant_digit = 3LL ;
		eastward _stokes_drift_raw_15m:units = "cm/s" ;
		eastward _stokes_drift_raw_15m:comment = "optionnelle" ;
	float northward _stokes_drift_full_0m (n_posneg, n_box) ;
```

```
		northward _stokes_drift_full_0m:_FillValue = 9.96921e+36f ;
		northward _stokes_drift_full_0m:long_name = "Northward Stokes drift estimated at 0m depth from the extended spectrum: SWIM spectrum ([22.5- 500] wavelength range) completed by an Elfouhaily modelling for largest wave numbers." ;
		northward _stokes_drift_full_0m:least_significant_digit = 3LL ;
		northward _stokes_drift_full_0m:units = "cm/s" ;
		northward _stokes_drift_full_0m:comment = "optionnelle" ;
	float eastward _stokes_drift_full_0m (n_posneg, n_box) ;
		eastward _stokes_drift_full_0m:_FillValue = 9.96921e+36f ;
		eastward _stokes_drift_full_0m:long_name = "Eastward Stokes drift estimated at 0m depth from the extended spectrum: SWIM spectrum ([22.5- 500] wavelength range) completed by an Elfouhaily modelling for largest wave numbers." ;
		eastward _stokes_drift_full_0m:least_significant_digit = 3LL ;
		eastward _stokes_drift_full_0m:units = "cm/s" ;
		eastward _stokes_drift_full_0m:comment = "optionnelle" ;

float northward _stokes_drift_full_15m (n_posneg, n_box) ;
		northward _stokes_drift_full_15m:_FillValue = 9.96921e+36f ;
		northward _stokes_drift_full_15m:long_name = "Northward Stokes drift estimated at 15m depth from the extended spectrum: SWIM spectrum ([22.5- 500] wavelength range) completed by an Elfouhaily modelling for largest wave numbers." ;
		northward _stokes_drift_full_15m:least_significant_digit = 3LL ;
		northward _stokes_drift_full_15m:units = "cm/s" ;
		northward _stokes_drift_full_15m:comment = "optionnelle" ;
	float eastward _stokes_drift_full_15m (n_posneg, n_box) ;
		eastward _stokes_drift_full_15m:_FillValue = 9.96921e+36f ;
		eastward _stokes_drift_full_15m:long_name = "Eastward Stokes drift estimated at 15m depth from the extended spectrum: SWIM spectrum ([22.5- 500] wavelength range) completed by an Elfouhaily modelling for largest wave numbers." ;
		eastward _stokes_drift_full_15m:least_significant_digit = 3LL ;
		eastward _stokes_drift_full_15m:units = "cm/s" ;
		eastward _stokes_drift_full_15m:comment = "optionnelle" ;


// global attributes:
		:platform = "CFOSAT" ;
		:sensor = "SWIM" ;
		:institution = "CNES" ;
		:contact = "aollivier@groupcls.com, maverseng@groupcls.com" ;
		:ars = 5.6f ;
		:dphi = 15.f ;
		:cycle = "033_2019-12-22T10:15:55Z_2020-01-04T10:16:21Z" ;
		:wlmin = "30.f" ;
		:wlmax = "500.f" ;
		:product_version = "1.0" ;
		:software_version = "production_l2pder: 2.7.1" ;
		:creation_date = "2024-11-04T09:07:43" ;
		:processing_level = "L2PDER" ;
		:oper_version = "OP06" ;
		:Conventions = "CF-1.6" ;
		:wave_spectra_beam = "10" ;
		:comment = "Added value products from SWIM nadir and off-nadir beams and averaged by box." ;
		:first_meas_time = "2020-01-01 02:14:28" ;
		:last_meas_time = "2020-01-01 03:48:44" ;
}
```

8.2 SWIM surface Stokes drift map

The surface Stokes drift was estimated for SWIM cycle 76 (July 2023) and compared to MFWAM Stokes drift. Results are presented on Figure 14.

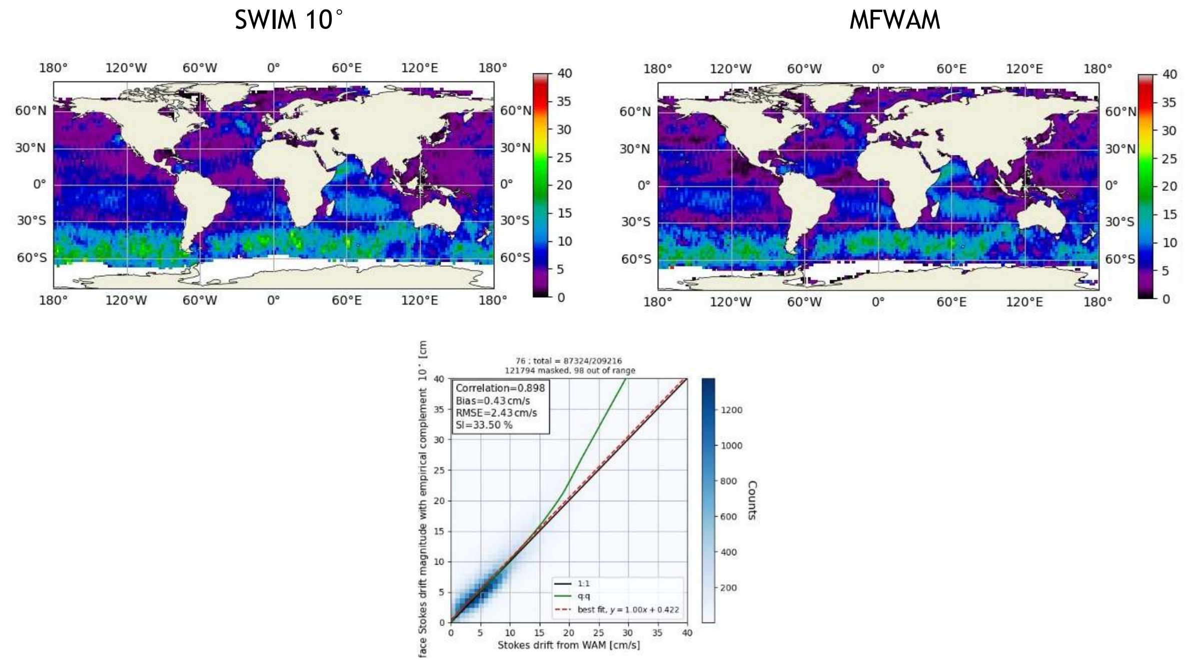

Figure 14: comparative maps of SWIM and MFWAM surface Stokes drift magnitude (cm/s) and corresponding scatter plot.

9 Bibliography

Breivik, O. B. (2016). A Stokes drift approximation based on the Phillips spectrum. *Ocean Modelling*, 49-56.

Breivik, O. J. (2014). Approximate Stokes Drift Profiles in Deep Water. *J. Phys. Oceanogr.*, 2433-2445.

Hauser D. et al., (2017). SWIM: The first spaceborne wave scatterometer, IEEE Trans. Geosci. Remote Sens., vol. 55, no. 5, pp. 3000–3014, May 2017, doi: 10.1109/TGRS.2017.2658672., https://hal-insu.archives-ouvertes.fr/insu-01456490/document

Hauser D. et al., (2021). New Observations From the SWIM Radar On-Board CFOSAT: Instrument Validation and Ocean Wave Measurement Assessment, in IEEE Transactions on Geoscience and Remote Sensing, vol. 59, no. 1, pp. 5-26, Jan. 2021, doi: 10.1109/TGRS.2020.2994372, https://hal-insu.archives-ouvertes.fr/insu-02324383v2/document

Elfouhaily, T. C. (1997). A unified directional spectrum for long and short wind-driven waves. *J. Geophys. Res.*, 15,781-15,796.

Kenyon, K. (1969). Stokes Drift for Random Gravity Waves. *J. Geophys. Res., 74*(28), 6991-6994.

Mitsuyasu, H. e. (1975). Observations of the Directional Spectrum of Ocean Waves Using a Cloverleaf Buoy. *J. Phys. Oceanogr.*, 750-760.

Peureux, C. (2018). Note on the directional properties of meter-scale gravity waves. *Ocean Science*.

Peureux et al., (2021). SWIM ocean waves spectra, illustration of performance, https://cfosatst.aviso.altimetry.fr/fileadmin/user_upload/CFOSAT2021/presentations/P-CFOSAT2021-857.pdf

Phillips, O. M. (1958). The equilibrium range in the spectrum of wind-generated waves. *J. Fluid Mech.*, 426.

Pierson, W. J. (1964). A proposed spectral spectral form for fully develop wind-sea based on the similarity of S. A. Kitaigorodskii. *J. Geophys. Res.*, 5181-5190.